



 Cite this: *RSC Adv.*, 2020, 10, 26151

Optimization extraction and characterization of *Artemisia ordosica* polysaccharide and its beneficial effects on antioxidant function and gut microbiota in rats

 Y. Y. Xing, Y. Q. Xu, X. Jin, L. L. Shi, S. W. Guo, S. M. Yan and B. L. Shi *

In this study, a novel polysaccharide was isolated from *Artemisia ordosica* by water-extraction-ethanol-precipitation method. The optimal extraction conditions of *Artemisia ordosica* polysaccharide (AOP) were determined by single factor investigation and response surface methodology optimization, and were shown as follows: a liquid–solid ratio of 15.4 : 1 mL g⁻¹, extraction time of 4.3 h, extraction temperature of 60 °C. Under the optimal conditions, the extraction yield and the sugar content of the AOP were 5.56% and 52.65%. Gel permeation chromatography coupled to multi-angle laser light scattering, a refractive index detection system and ion-exchange chromatography were used to determine the characterization of AOP. These results indicated that AOP, with a molecular weight of 2.1 kDa (62.6%) and 1.5 kDa (37.4%), had narrow polydispersity and rod conformations, and was composed of arabinose, galactose, glucose, xylose, mannose, galacturonic acid and glucuronic acid with molar ratio of 6.87 : 10.67 : 54.13 : 2.49 : 18.37 : 4.83 : 2.64 : 2.64. In addition, AOP exerted antioxidant ability *in vitro* and *in vivo* (rats). Moreover, AOP significantly modulated the composition of cecal microbiota population. Therefore, AOP is expected to be a functional ingredient for health improvement through improving antioxidant ability and modulating gut health.

Received 8th June 2020

Accepted 3rd July 2020

DOI: 10.1039/d0ra05063f

rsc.li/rsc-advances

1. Introduction

Artemisia species are one of the most popular plants in Chinese traditional herbal medicine and frequently used in diseases treatment such as malaria, hepatitis, cancer, inflammation and infections by fungi, bacteria and viruses.¹ Among genus *Artemisia* plants, *Artemisia ordosica*, a perennial herb, is one of the main shrubs growing in north and northwest areas in China. Owing to rich nutrients and bio-active components, *Artemisia ordosica* and their extracts can be used as natural Chinese herbal medicine feed additives. Our previous study demonstrated the growth promoting and immune regulatory effect of water extracts from *Artemisia ordosica* on broilers and piglets.^{2,3} However, the specific compounds of *Artemisia ordosica* water extracts that have the anti-inflammatory and antioxidant effect remain unclear.

Recently, the components of water extracts from *Artemisia ordosica* were identified, which were comprised four main chemical components, including alcohols, phenols, organic acids and saccharides.⁴ Due to their nontoxic properties and pharmacological activities, including antioxidation, immunomodulation, antitumor, anti-inflammation, inhibition of cardiovascular and cerebrovascular disease, the polysaccharides

extracted from herb plants have attracted increasing attention.^{5–7} Furthermore, polysaccharides were recently extracted from *Artemisia argyi* and their immunomodulatory activity and antioxidant activity were confirmed.^{8,9} Moreover, growing evidences have indicated that polysaccharide has prebiotic potential through altering the composition and abundance of beneficial gut microbiota. It has shown that the gut microbiota plays a critical role in nutrient uptake, utilization, and metabolism, which may contribute to metabolic diseases.^{10–12}

Hence, based on our previous study of *Artemisia ordosica* in animals^{2,3} and the findings of other researchers, we hypothesized that *Artemisia ordosica* polysaccharide (AOP) in diets could affect antioxidative capacity and gut microbiota in animals and further exploration is imperative. The objective of this study was to investigate the optimized extraction conditions of AOP. After that, the antioxidative capacity of AOP *in vitro* and *in vivo* was investigated. In addition, the effects of AOP on gut microbe structure in rats were researched as well. The results may ultimately contribute to the developing and application for AOP.

2. Materials and methods

2.1. Preparation of AOP

Artemisia ordosica was collected from Erdos (Inner Mongolia, China) in July. The AOP was prepared by using water-extraction-

College of Animal Science, Inner Mongolia Agricultural University, Hohhot 010018, China. E-mail: shibinlin@yeah.net



ethanol-precipitation method. Briefly, the whole plant (without root) was washed with distilled water and placed in the shade to dry at room temperature. The whole dried plant was grounded into powders to pass through a 60-mesh sieve. The powder of *Artemisia ordosica* firstly degreased by petroleum ether in the Soxhlet apparatus for 12 h. Then 200 g of *Artemisia ordosica* powder was steeped in 3.08 L distilled water for 4.3 h under 60 °C. The aqueous extract was filtered through a 0.45 μm filter and concentrated to 1/5 of the original volume. Anhydrous ethanol was added to the concentrated supernatants (ratio 4 : 1, v/v) for precipitation of polysaccharide for 48 h at 4 °C. The sediment was collected by centrifugation (12 000 × g, 15 min) and washed successively with petroleum ether, acetone, and ethanol. Then the sediment was dissolved in water and deproteinated twice with Sevag reagent (*n*-butyl alcohol : chloroform = 1 : 4). Afterward, the supernatant was collected and dialyzed using a biological semipermeable membrane (molecular weight cutoff: 500 Da, Beijing Solarbio Science and Technology Co., Ltd., Beijing, China) against distilled water at 4 °C for 48 h, with changing the distilled water every 12 h. The resulting solution was lyophilized by a vacuum evaporate to prepare the powder, and stored at −20 °C until use. The total carbohydrate content was measured by using the phenol–sulfuric acid method using glucose as the standard.¹³ The protein content was determined by Coomassie brilliant blue method using bovine serum albumin as the standard.¹⁴ The polyphenols content was accomplished by Folin–Ciocalteu reagent assay using gallic acid as the standard.¹⁵ The uronic acid content was evaluated using glucuronic acid as a standard.¹⁶

2.2. Single factor evaluation

Extraction liquid–solid ratio, temperature and time were set as factors to evaluate their influences on the AOP yield. There were five treatments with six replicates of each factor, and each factor was investigated individually.

2.3. Response surface methodology optimization

Based upon the single-factor experimental results, three-factor (extraction liquid–solid ratio, temperature, and time) with three-level response surface analysis was performed to obtain the maximum AOP yield using Box–Behnken design (BBD) combined with response surface methodology (RSM).

2.4. Characterization of polysaccharide

2.4.1 Determination of average molecular weight of AOP. The AOP water solution (5 mg mL^{−1}) was heated at 100 °C for 5 min and centrifuged at 12 000 × g for 10 min to collect the supernatant. Gel permeation chromatography (GPC) coupled to multi-angle laser light scattering (MALLS; Heleos, Wyatt Technology Corp., Santa Barbara, CA, USA), and a refractive index (RI; model RI-150; Thermo Electron Corp., Yokohama, Japan) detection system (GPC-MALLS-RI system) was used to determine the average molecular weight of AOP. The mobile phase of the GPC-MALLS-RI was 0.1 M NaNO₃ with 0.02% (w/v) Na₂S₂O₃ at a flow rate of 0.4 mL min^{−1} and column oven temperature was set at 60 °C. The value of refractive index increment (dn/dc) was

0.14 mL g^{−1}. The injection volume was 20 μL. The *M_w*, polydispersity (*M_w*/*M_n*) and root mean square (RMS) radius were calculated.

2.4.2 Monosaccharide composition of AOP. The AOP sample (5 mg) was dissolved in 2 M trifluoroacetic acid (TFA, 4 mL) in a sealed tube, and kept at 121 °C for 2 h to complete hydrolysis. The excess TFA was removed by rotary evaporation. The residue was re-dissolved in methanol (2 mL) and dried with nitrogen using nitrogen blowing instrument for three times. Then the residue was re-dissolved in ultrapure water in chromatographic bottle and measured by ion-exchange chromatography (Dionex ICS 5000) equipped with a Carbo-Pac PA20 analytic column (250 × 4 mm; Dionex). Gradient elution was carried out according to the following process: 0–25 min, 1% 500 mM NaOH; 25.1–40 min, 10% 500 mM NaOH and 90% ultrapure water; and 40.1–50 min, 100% 500 mM NaOH. All procedures were conducted at a constant flow rate of 0.5 mL min^{−1} at a column temperature of 30 °C. The injection volume was 20 μL. Fucose, arabinose, galactose, glucose, xylose, mannose, fructose, ribose, galacturonic acid and glucuronic acid were used as the monosaccharide standards.

2.5. Antioxidative activity assay for AOP

2.5.1 Assay of DPPH free radical scavenging activity. The DPPH free radical scavenging activity of AOP was performed by spectroscopic method.¹⁷ Briefly, various concentrations (0.0, 0.2, 0.4, 0.6, 0.8 and 1.0 mg mL^{−1}) of AOP were added into ethanol containing DPPH. The reaction mixture was shaken vigorously and the absorbance of remaining DPPH was measured at 517 nm after 30 min at room temperature in dark. Vitamin C (Vc) was used as positive control. The samples were analyzed in triplicate. DPPH free radical scavenging activity of AOP was calculated according to the following equation:

$$\text{DPPH free radical scavenging ability (\%)} = [1 - (A_1 - A_2)/A_0] \times 100\%$$

In the equation, *A*₁ was the absorbance of AOP samples; *A*₂ was the absorbance of the samples under conditions as *A*₁ with distilled water instead of DPPH; *A*₀ was the absorbance of the distilled water instead of samples.

2.5.2 Assay of hydroxyl radical scavenging activity. Hydroxyl radical scavenging activity of AOP was evaluated by the reported method.¹⁷ In brief, 500 μL of FeSO₄ (9.0 mM), 500 μL of H₂O₂ (8.8 mM) with 500 μL of AOP at the concentrations of 0.0, 0.2, 0.4, 0.8 and 1.0 mg mL^{−1}, respectively, were mixed to react for 10 min at 25 °C, then the mixture was mixed with 500 μL salicylic acid ethanol (9.0 mM), and the absorbance at 510 nm was measured after reaction at 25 °C for 30 min. Vc was used as positive control. The samples were analyzed in triplicate. Hydroxyl radical scavenging ability of AOP was calculated according to the following equation:

$$\text{Hydroxyl radical scavenging ability (\%)} = [1 - (A_1 - A_2)/A_0] \times 100\%$$

In the equation, A_1 was the absorbance of AOP samples; A_2 was the absorbance of the samples under conditions as A_1 with distilled water instead of FeSO_4 ; A_0 was the absorbance of the distilled water instead of samples.

2.5.3 Assay of ABTS free radical scavenging activity. ABTS radical scavenging activity of AOP was evaluated according to the reported method.¹⁷ ABTS solution (200 μL) was mixed with 20 μL of different concentrations of AOP solution (0.0, 0.2, 0.4, 0.6, 0.8 and 1.0 mg mL^{-1}) into a 96-well plate. The absorbance at 734 nm was measured after reaction for 6 min at 25 °C. Vc was used as positive control. The samples were analyzed in triplicate. The radical scavenging activity was determined by comparing the absorbance with which of blank (100%) containing only ABTS and solvent.

2.5.4 Reducing power assay. The reducing power (RP) was evaluated by the method according to Wan *et al.* (2016)¹⁸ with some modifications. Briefly, each sample (0.75 mL) was blended with PBS (200 mM, pH 6.6, 0.75 mL) and 1% potassium ferricyanide (0.75 mL). After incubation for 20 min at 50 °C, the mixed solution was added 10% trichloroacetic acid (0.75 mL), then centrifuged at 1500 $\times g$ for 10 min. The supernatant (1.5 mL) was subsequently mixed with distilled water (1.5 mL) and 0.1% ferric chloride (0.4 mL). The absorbance at 700 nm of the solution was measured. An increased absorbance of the sample indicated increased reducing power.

2.6. Animals and experimental protocol

Male Wistar rats were obtained from Experimental Animal Center of Inner Mongolia Medical University (Hohhot, China). Twelve rats were randomly divided into two groups ($n = 6$ per group), each group was supplied experimental diet which was the basal diet contained (1) no additive (CON) or (2) 300 mg per kg AOP for 21 days. During the entire experimental period, all rats were fed a standardized pellet feed and water *ad libitum* and housed under standard laboratory conditions with a constant 12 h light and 12 h dark at room temperature maintained at 23 ± 1 °C. All rats were individually weighed on day 1 and day 21, after the fasting for 12 h. Feed intake and diet residue of each rat was weighed daily. Average daily body weight gain (ADG), average daily feed intake (ADFI) and the ratio of feed to gain (F/G) were calculated.

By the end of the study, the rats were starved for 12 h and then sacrificed for blood collection and tissue sampling under anesthesia using sodium pentobarbital. Serum sample was separated by centrifugation at 3000 $\times g$ for 10 min and stored at -20 °C until analysis. Liver samples and cecal content were frozen in liquid nitrogen and stored at -80 °C until analysis. The levels of alanine aminotransferase (ALT), aspartate aminotransferase (AST) and alkaline phosphatase (ALP) in the serum were determined by the automatic analyzer (HITACHI 747, Tokyo, Japan). All animal procedures were performed in accordance with the National Standard Guideline for Ethical Review of Animal Welfare (GB/T 35892-2018) and approved by the Animal Care and Use Committee of Inner Mongolia Agricultural University.

2.6.1 Assay of antioxidant indices in serum and tissue samples. Liver tissue was minced and homogenized (10% w/v) in saline, then centrifuged at 3000 $\times g$ for 10 min at 4 °C. The resulting supernatant and serum were used to determine total antioxidant capacity (T-AOC), enzymes activities including catalase (CAT), superoxide dismutase (SOD) and glutathione peroxidase (GPx), and the indicator of lipid peroxidation malondialdehyde (MDA). Antioxidant indexes and protein were measured by commercially available kits (Nanjing Jiancheng Bioengineering Institute, Nanjing, China). Data were expressed as U per mg of protein for tissues and U mL^{-1} for serum. All procedures were conducted in accordance with the manufacturer's instructions.

2.6.2 RNA preparation and fluorescence quantitative real-time PCR. Total RNA in liver tissue was isolated by using the Trizol extraction method according to the manufacturer's instructions. RNA was quantitatively and qualitatively determined by using an ultraviolet spectrophotometer at 260 nm and 280 nm. RNA integrity was analyzed by using horizontal electrophoresis through 1.5% agarose gel. Genomic DNA contamination was removed by using DNase provided with the kit. Synthesis of cDNA was conducted with the PrimeScript^{RT} reagent Kit with gDNA Eraser (Takara Bio Inc., Otsu, Japan) according to the manufacturer's instructions. The quantitative real-time PCR (qPCR), with the help of TB Green (TB Premix Ex Taq II, Perfect Real Time, Takara Bio Inc.) according to the manufacturer's instructions, was performed on an Illumina real-time PCR machine in two steps: a cycle of initial denaturing

Table 1 Primer sequences and parameter

Genes	GenBank no.	Primer sequences (5'-3')	Length (bp)	T_a (°C)
β -Actin	NM_031144.2	F. CCTAAGGCCAACCGTGAAAA R. CAGAGGCATACAGGGACAACAC	103	60
CAT	NM_012520.2	F. GAACATTGCCAACCCACTGAAAG R. GTAGTCAGGGTGGACGTCAGTGAA	85	60
GPx1	NM_001037471	F.CTTCCCAATCTGCCCTACTTA R.CTCCTCCTCTGTCTCTCCACAC	112	60
SOD1	NM_017050.1	F. GGCAAAGGTGGAAATGAAGAAA R. CAGTTTAGCAGGACAGCAGATGAG	136	60
SOD2	NM_174294	F. CCAGGAGCAAACCAAGAAC R. TGCAACTGGTTTCTGTTGGT	148	60

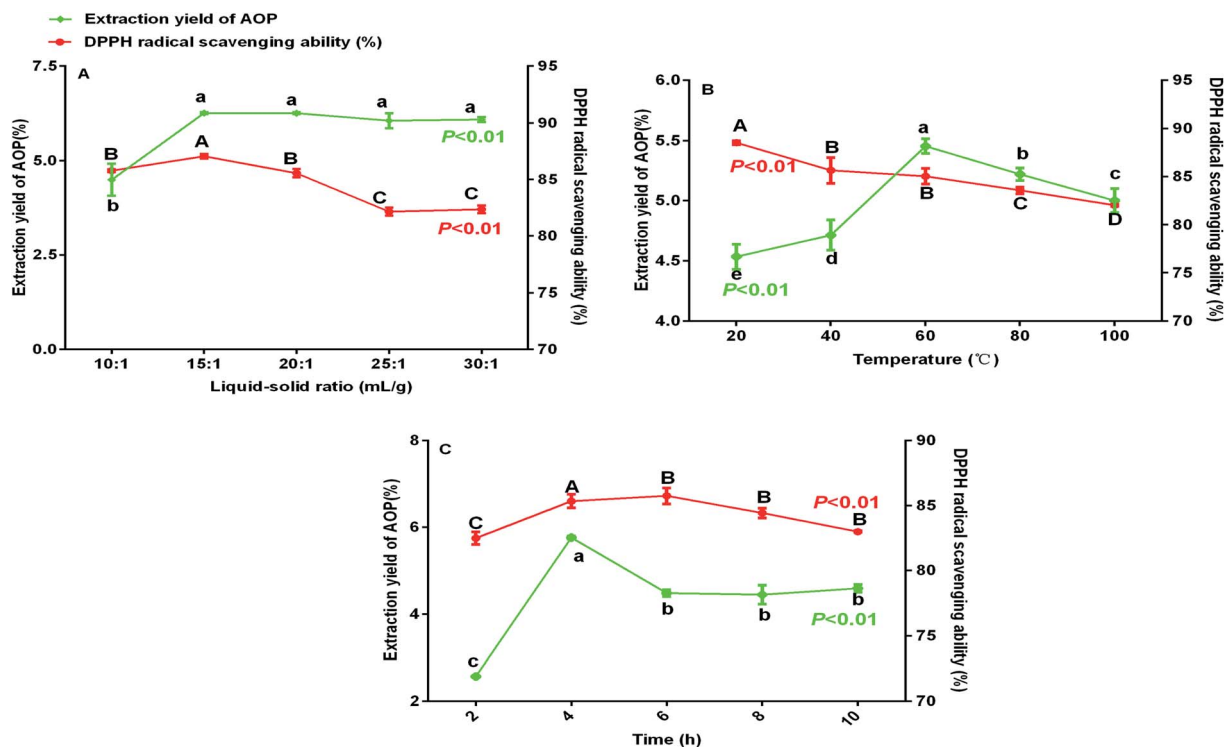


Fig. 1 Extraction yield and DPPH radical scavenging ability (%) of AOP under different extraction conditions (A: liquid–solid ratio, B: temperature and C: time).

at 95 °C for 30 s, followed by 40 cycles involving denaturation at 95 °C for 5 s and annealing at 60 °C for 30 s. A subsequent dissociation stages produced a melting curve to verify the specificity of the amplified products. The target genes including *CAT*, *GPx*, *SOD1*, *SOD2* and their primer sequences are tabulated in Table 1, which were designed by Shanghai Sangon Biotech (Shanghai, China). β -Actin was used as reference gene and the relative fold difference in the mRNA expression levels was calculated using the $2^{-\Delta\Delta C_T}$.

2.6.3 DNA extraction and MiSeq sequencing. Cecal contents genomic DNA was extracted using the EZNA® Soil NDA Kit (Omega Bio-Tek, Inc., GA, USA) in accordance with kit protocols. The resulting DNA was amplified with specific bacterial primers targeting the V3–V4 hypervariable region of the bacterial 16S rRNA using universal primers: 338F (5-*ACTCCTACGGGAGGCAGCAG*-3), and 806R (-*GGACTACHVGGGTWCTAAT*-3). PCR reactions were performed on a thermocycler PCR system in following steps: 95 °C for 180 s; followed by 40 cycles involving 95 °C for 30 s, 60 °C for 30 s, 72 °C for 45 s; then 72 °C for 10 min. The PCR products were checked on a 2% agarose gel and purified according to the manufacturer's instructions. The amplicons were purified using the AxyPrep DNA Gel Extraction Kit (Axygen Biosciences, Union City, USA) and quantified using QuantiFluor™-ST fluorometer (Promega, Madison, USA), and then sequenced on a MiSeq platform (Illumina, San Diego, USA) according to the protocols in a Shanghai MajorBio Bio-Pharm Technology Co. Ltd (Shanghai, China).

2.7. Statistical analysis

Values were expressed as mean \pm standard deviation (SD). The one-way analysis of variance (ANOVA) and Student's *t* test were used to detect significant differences. Values of $P < 0.05$ are considered to be statistically significant.

3. Results and discussion

3.1. BBD and RSM optimization

Previous study indicated that water-extraction-ethanol-precipitation method of plant polysaccharide is commonly used for its economical nature, convenient use and is strongly related to extraction liquid–solid ratio, time and temperature.¹⁹ In addition, polysaccharide yield and activities may reduce due to the excessive extraction time or temperature.²⁰ Hence, polysaccharide yield and DPPH radical scavenging ability (%) under different extraction conditions (liquid–solid ratio, temperature and extraction time) were determined to obtain the maximum

Table 2 Levels and factors of response surface design

Factors	Levels		
	–1	0	1
A: liquid–solid ratio (mL g^{-1})	10 : 1	15 : 1	20 : 1
B: temperature (°C)	40	60	80
C: times (h)	2	4	6

Table 3 Box–Behnken design and response for extraction yield of AOP

Run	Independent variable			Response
	A (liquid–solid ratio, mL g ⁻¹)	B (temperature, °C)	C (time, h)	Extraction yield (%)
1	15 : 1	40	2	3.65
2	10 : 1	60	6	3.10
3	15 : 1	60	4	5.50
4	15 : 1	80	6	3.00
5	15 : 1	40	6	3.20
6	20 : 1	80	4	3.50
7	15 : 1	60	4	5.70
8	10 : 1	60	2	3.70
9	20 : 1	60	6	4.14
10	20 : 1	60	2	2.80
11	15 : 1	60	4	5.90
12	10 : 1	80	4	3.10
13	15 : 1	60	4	6.00
14	15 : 1	60	4	6.10
15	10 : 1	40	4	2.80
16	15 : 1	80	2	3.43
17	20 : 1	40	4	3.40

yield without decreasing antioxidant ability. As shown in Fig. 1, the maximum yield of polysaccharide was obtained at the liquid–solid ratio of 15 : 1 (Fig. 1A), temperature of 60 °C (Fig. 1B) and extraction time of 4 h (Fig. 1C). Of note, in the present study, the extraction yield of AOP significantly increased with the increase of extraction temperature from 20 to 60 °C and significantly decreased when the extraction temperature increased from 60 to 100 °C. An increasing extraction temperature could increase the molecular movement, resulting in accelerating the transfer of intracellular substances from the cells.²¹ However, higher temperature can cause the degradation of some thermo-sensitive materials, such as polysaccharide, resulting in declined yield.²² In addition, DPPH radical scavenging ability (%) was higher under this condition as well (Fig. 1A–C). Therefore, a liquid–solid ratio of 10 : 1–20 : 1, a temperature range between 40–80 °C and an extraction time of 2–6 h was selected for the BBD (Table 2). The experimental scheme was arranged by BBD and experimental results were shown in Table 3. The response surface plots and contour plots between the factors and AOP yield were shown in Fig. 2A–F, which depicted the interactions between two variables by keeping the other variables at their zero levels for AOP yield. The shapes of the contour plots, circular or elliptical, indicate whether the mutual interactions between variables are significant or not.²³ In addition, the analysis of variance was conducted and detailed in Table 4. From Fig. 2 and Table 4, it could be seen that two interaction coefficients (A and C) and all quadratic term coefficients (A^2 , B^2 and C^2) were significant with low P values ($P < 0.05$). Moreover, the model was highly significant (Table 4), which indicated that the predicted model more highly illustrated the pattern of the interactions between variables.²⁴

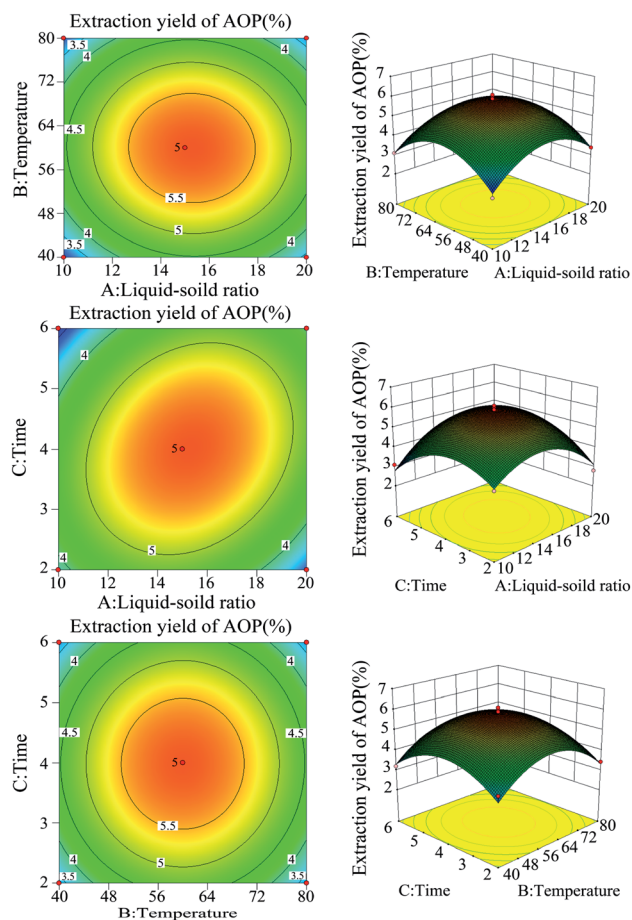


Fig. 2 The response surface plots and contour plots between the factors and AOP yield.

By applying multiple regression analysis on the experimental data, the quadratic fitting linear regression equation for AOP extraction was as follows: $Y = -20.3751 + 1.37973A + 0.41990B + 1.53956C - 0.0005AB + 0.0448475AC + 0.0001625BC - 0.050505A^2 - 0.00344344B^2 - 0.28566C^2$, where Y denotes AOP extraction yield (%), A denotes the liquid–solid ratio (mL g⁻¹), B denotes the extraction temperature (°C), and C denotes the extraction time (h). The variance of the quadratic regression model showed that the determination coefficient (R^2) was 0.9309, indicating that the calculated model was able to explain 93.09% of the result in the case of AOP yield.²⁵ The optimum extraction conditions of AOP were as follows: liquid–solid ratio of 15.39 : 1; extraction time of 4.28 h and extraction temperature of 59.96 °C. The prediction yield of AOP was estimated to be up to 5.84%. The extraction experiment was repeated three times under the optimal extraction condition (4.3 h, 60 °C, and liquid–solid ratio of 15.4 : 1) to verify the reliability of the results, and the extractive rate of AOP was 5.56% (Table 5), which was very close to the predicted value. It was suggested that the optimum conditions for AOP extraction could be effectively performed in practice. The carbohydrate content, protein content, uronic acid content and phenolic content for AOP were 52.65%, 2.39%, 4.27% and 0.11% (Table 5).

Table 4 Analysis of variance of the regression model

Source	Sum of squares	df	Mean square	F value	P-value
Model	23.67	9	2.63	24.96	0.0002
A-liquid-soild	0.16	1	0.16	1.54	0.2547
B-temperature	8.45×10^{-5}	1	8.45×10^{-5}	8.019×10^{-4}	0.9782
C-time	2.485×10^{-3}	1	2.485×10^{-3}	0.024	0.8823
AB	0.01	1	0.01	0.095	0.7670
AC	0.94	1	0.94	8.92	0.0203
BC	1.690×10^{-4}	1	1.690×10^{-4}	1.604×10^{-3}	0.9692
A ²	6.71	1	6.71	63.70	<0.0001
B ²	7.99	1	7.99	75.81	<0.0001
C ²	5.50	1	5.50	52.17	0.0002
Residual	0.74	7	0.11		
Lack of fit	0.51	3	0.17	2.91	0.1647
Pure error	0.23	4	0.058		
Cor total	24.41	16			

Table 5 Extraction yields and chemical components analysis of AOP

	Extraction yield (%)	Carbohydrate (%)	Protein (%)	Uronic acid (%)	Phenolic (%)
AOP	5.56 ± 0.41	52.65 ± 5.23	2.39 ± 0.09	4.27 ± 0.49	0.11 ± 0.002

3.2. Molecular characteristics of polysaccharide

The RI-MALS superimposed chromatograms for the AOP are shown in Fig. 3. As shown in the RI chromatogram, the

polysaccharide had two major peaks at the elution time of 69–71 min and 72–73 min (Fig. 3A). Hence, the average M_w value of AOP were 2.1 kDa (62.6%) and 1.5 kDa (37.4%). Previous studies

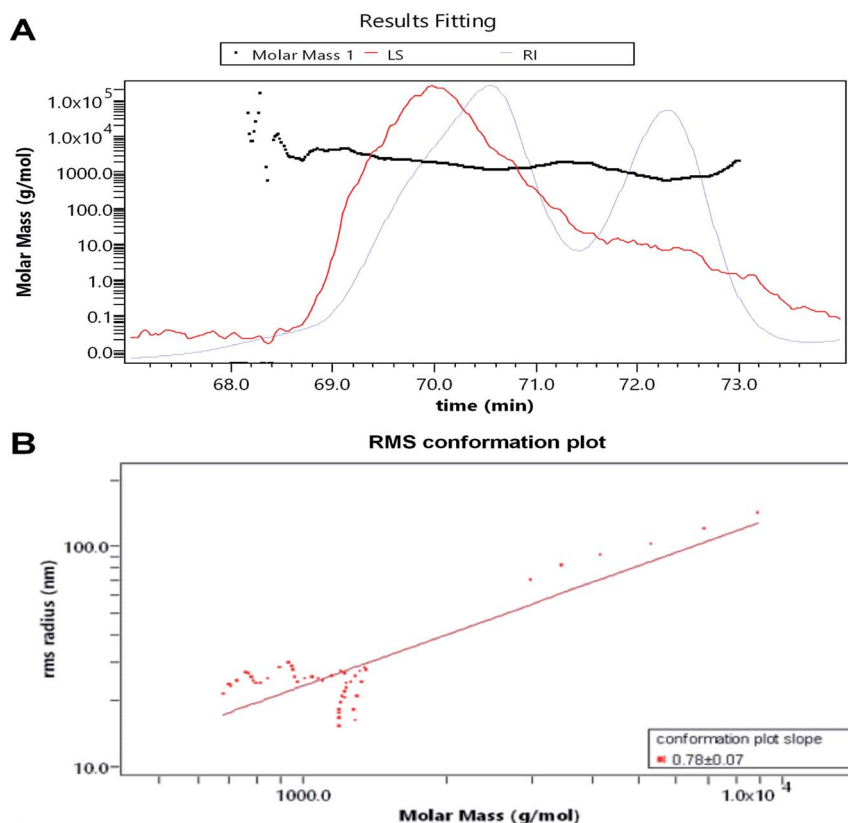


Fig. 3 Average molecular weight of AOP obtained from GPC-MALS-RI. (A) average molecular weight; (B) root mean square conformation plot.

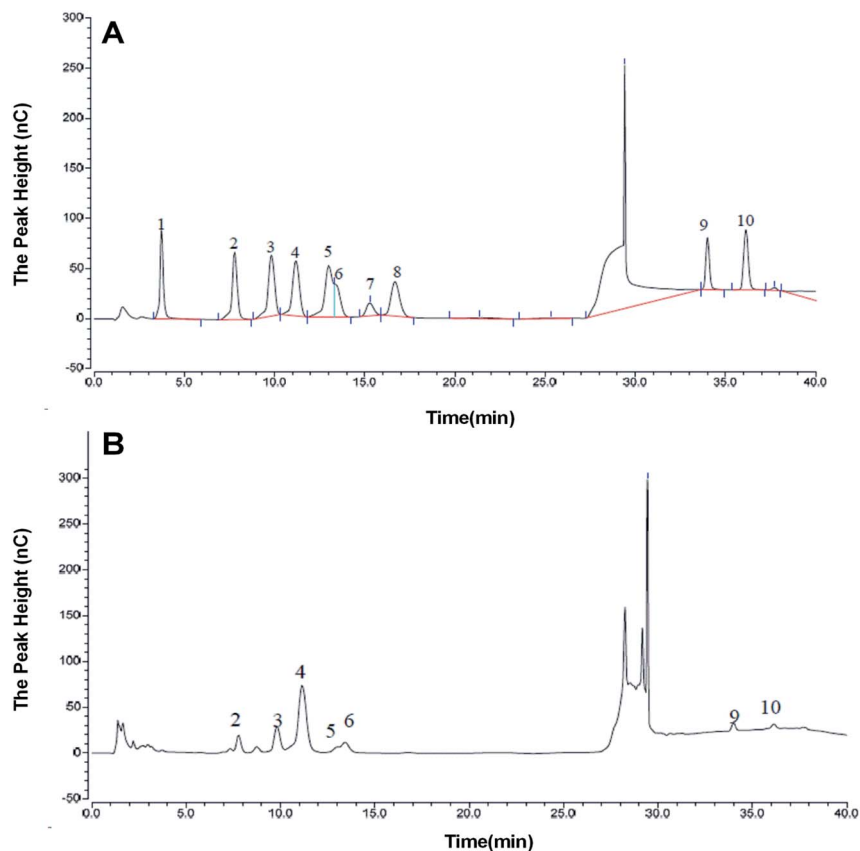


Fig. 4 Monosaccharide composition of AOP obtained from ion chromatography. ^{a,b} (A) Monosaccharide standards; (B) AOP.

reported that molecular weight was strongly related to the viscosity and solubility of polysaccharide solution. High molecular weight polysaccharide generally shares a number of characteristics with high viscosity and poor solubility, which limits its application.^{26,27} Thus, AOP with moderate molecular weight would be favorable for its application. The AOP also had narrow polydispersity (PD = 1.058 and 1.063), close to 1, which indicated that AOP was homogeneity.²⁸ The conformation plot of $\log R_g - \log M_w$ indicated the rod conformations was adopted for AOP with a slope of 0.78 (Fig. 3B). The value of the line slope when plotting $\log R_g$ versus $\log M$ can be used to obtain conformational information of polymers in solution, e.g., the value of ν is approximately 0.3 for hard sphere conformation, approximately 0.5 for random coil, and approximately 1 for rigid rod.^{29,30} The conformation plot of $\log R_g - \log M_w$ indicated the rigid rod conformations were adopted for AOP.

3.3. Monosaccharide composition assay

The monosaccharide composition of AOP was determined by ion chromatography. On the basis of the elution time of monosaccharide standards (Fig. 4A), the AOP composed of arabinose, galactose, glucose, xylose, mannose, galacturonic acid and glucuronic acid monohydrate with molar ratio of 6.87 : 10.67 : 54.13 : 2.49 : 18.37 : 4.83 : 2.64 : 2.64 (Fig. 4B). It has been reported that polysaccharide could modulate the composition and abundance of beneficial microbiota through

altering fermentation behavior, which is greatly influenced by their monosaccharide compositions (see following sections).³¹

3.4. Antioxidant activity of AOP *in vitro*

Plant polysaccharide is with powerful antioxidant capable of mopping up free radicals.³² DPPH radical is one of common radicals and usually used to evaluate the capacity of natural antioxidant.³³ The DPPH radical scavenging activities of AOP at different concentrations were shown in Fig. 5A. It could be seen that AOP showed dose-dependent radical scavenging capacity along with increasing concentration. At a concentration of 1.0 mg mL^{-1} , the DPPH radical scavenging activity for AOP was $58.60 \pm 1.59\%$ which was far lower than positive control (Vc).

Uncontrolled production of hydroxyl radical may cause damage to numerous biological substances, which led to diseases.³⁴ Thus, seeking a natural antioxidant to scavenge hydroxyl radical is obtained increasing attention. The scavenging effect of AOP on hydroxyl radical was determined (Fig. 5B). Concentration-dependent effect of radical-scavenging activity was observed. At a concentration of 1.0 mg mL^{-1} , the hydroxyl radical scavenging activity of AOP was $38.20 \pm 2.06\%$, which suggested a satisfying radical scavenging activity.

ABTS radical scavenging activity is an important index to evaluate the total antioxidant power of polysaccharide.¹⁷ The ABTS radical-scavenging effect of AOP was presented in Fig. 5C.

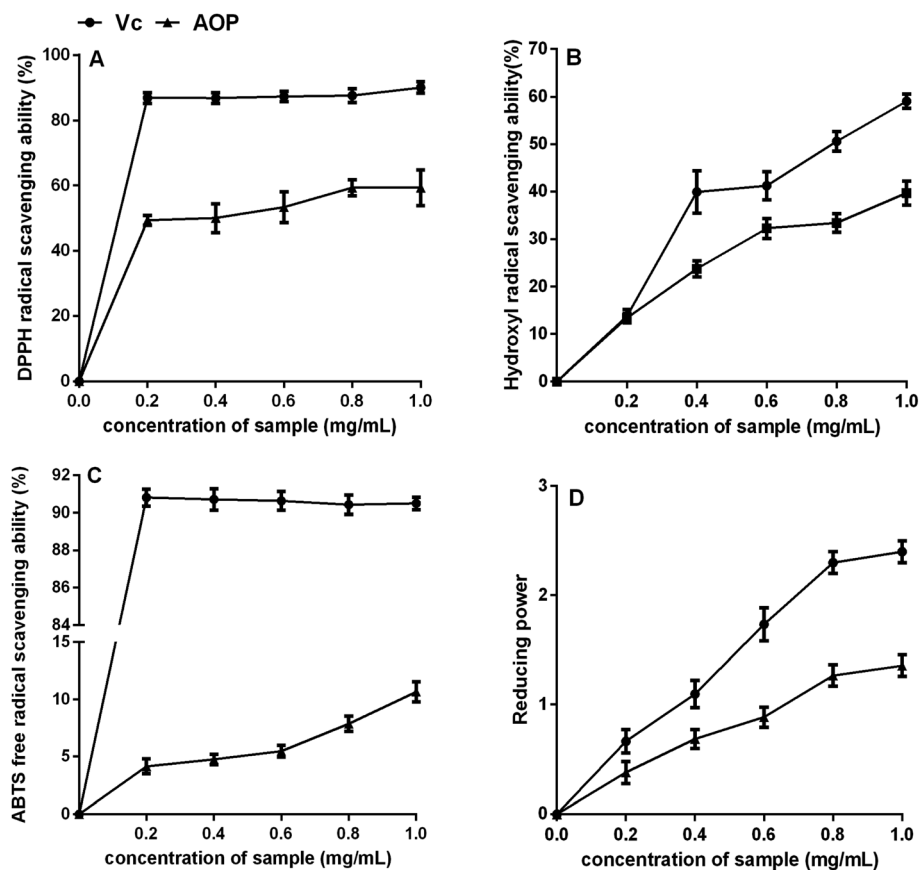


Fig. 5 Antioxidant activity of AOP *in vitro*. (A) DPPH radical scavenging activity; (B) hydroxyl radical scavenging activity; (C) ABTS radical scavenging activity; (D) reducing power.

Table 6 Effects of AOP on growth performance and serum biochemical indexes of rats^{a,b}

Items	CON	AOP	P-value
Growth performance			
ADG, g d ⁻¹	3.42 ± 0.89 ^B	4.20 ± 0.35 ^A	0.02
ADFI, g d ⁻¹	20.40 ± 0.36	20.61 ± 0.55	0.56
G : F, g g ⁻¹	0.16 ± 0.01 ^B	0.23 ± 0.02 ^A	0.002
Serum biochemical indexes			
ALT (U L ⁻¹)	92.42 ± 2.00	87.81 ± 1.94	0.14
AST (U L ⁻¹)	160.8 ± 20.38	133.3 ± 10.08	0.31
ALP (U L ⁻¹)	239.8 ± 9.62 ^A	144.5 ± 4.02 ^B	0.004

^a Different letter within the same line denote significant differences between diets. ^b ALT, alanine aminotransferase; AST, aspartate aminotransferase; ALP, alkaline phosphatase.

Concentration-dependent effect of radical scavenging activity was observed as well. Compared to Vc, AOP exhibited lower ABTS radical scavenging activity at all tested concentrations.

The reducing power of AOP was investigated and the results are shown in Fig. 5D. Both AOP and Vc demonstrated evident reducing effects in a concentration-dependent manner at concentration range of 0–1.0 mg mL⁻¹. The reducing power of

Table 7 Effects of AOP on serum and liver antioxidative activities and the corresponding gene expressions^a

Items	CON	AOP	P-value
Serum			
T-AOC, U mL ⁻¹	8.51 ± 0.67	9.49 ± 0.46	0.30
SOD, U mL ⁻¹	277.0 ± 2.76 ^B	302.3 ± 2.03 ^A	0.01
CAT, U mL ⁻¹	4.60 ± 0.09	5.39 ± 0.24	0.16
GPx, U mL ⁻¹	1810 ± 88.29 ^B	2216 ± 94.89 ^A	0.01
MDA, nmol mL ⁻¹	4.11 ± 0.21	4.49 ± 0.46	0.49
Liver			
T-AOC, U per mg prot.	1.69 ± 0.14 ^B	2.45 ± 0.33 ^A	0.09
SOD, U per mg prot.	259.1 ± 8.54 ^B	328.9 ± 23.37 ^A	0.04
CAT, U per mg prot.	45.81 ± 3.81 ^B	70.31 ± 1.06 ^A	0.001
GPx, U per mg prot.	244.1 ± 8.76 ^B	276.2 ± 7.00 ^A	0.03
MDA, nmol per mg prot.	6.367 ± 0.16	4.76 ± 0.70	0.14
Genes in liver			
SOD1	1.00 ± 0.00 ^B	1.48 ± 0.13 ^A	0.03
SOD2	1.00 ± 0.00 ^B	1.44 ± 0.06 ^A	0.002
CAT	1.00 ± 0.00 ^B	1.38 ± 0.10 ^A	0.04
GPx1	1.00 ± 0.00	1.17 ± 0.16	0.23

^a Different letter within the same line denote significant differences between diets.

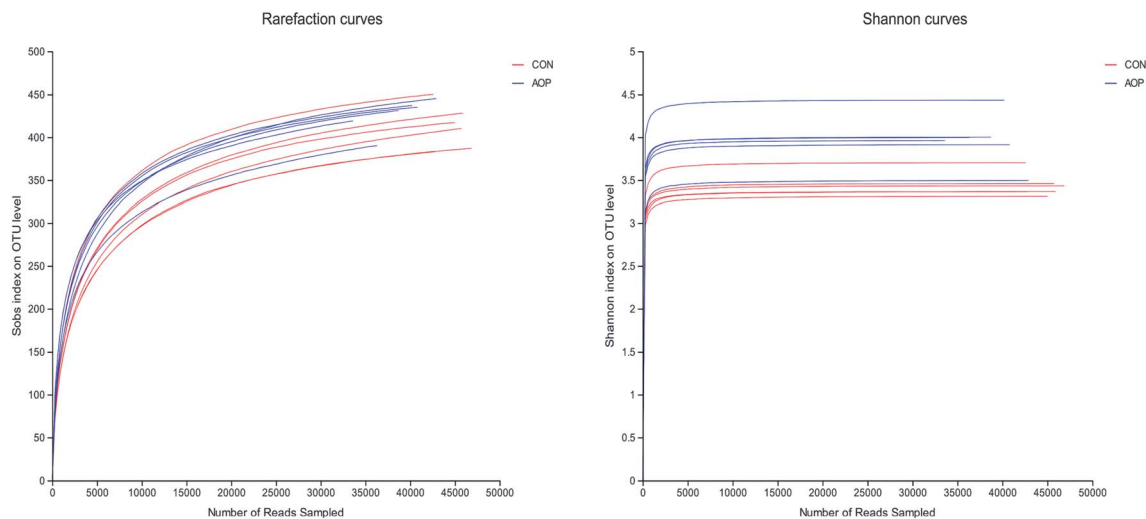


Fig. 6 The rarefaction and Shannon index curves.

the AOP was a little lower than that of Vc, but it was similar with *Artemisia annua* L. enzymatic treated,¹⁸ indicating that *Artemisia* species possessed antioxidant activity *in vitro*.

3.5. Growth performance of rats

As shown in Table 6, dietary supplementation with AOP significantly increased ADG and *G:F*. However, the effect of AOP on the ADFI was not detected ($P > 0.05$). Our previous study indicated that *Artemisia argyi* aqueous extract and *Artemisia annua* L. aqueous extract could improve growth performance of broilers.^{35,36} The present study was further confirmed the growth prompting effect of polysaccharide as the main component in the plant aqueous extract.

3.6. Hepatotoxicity of AOP

The effect of AOP on liver injury was evaluated by determining AST, ALT and ALP activities in serum. As shown in Table 6, the levels of serum ALT and AST activities did not affect by AOP feeding. AOP supplementation could significantly decrease ALP levels. ALP is intracellular and only a small amount is present in serum. The increasing ALP activity in serum, which is caused by the breakdown of cell in certain disease conditions, is the symptoms of hepatobiliary sickness.³⁷ Therefore, we can reasonably arrive at the suggestion that AOP is beneficial in protecting liver.

3.7. Antioxidative activities and gene expressions in serum and liver

Overproduction of free radicals in the body will cause damage to T cell, decrease immune function and bring cardiovascular and cerebrovascular disease risks.³⁸ Studies have found that some polysaccharides can not only inhibit above disease, but also inhibit lipid peroxidation, enhance the body's ability to scavenge free radicals and anti-aging.^{39,40} AOP is a highly promising source of antioxidants, which is confirmed in the present study by measuring scavenging ability to free radicals. Meanwhile, the antioxidant activities of AOP *in vivo*, including

lipid peroxidation indicator (MDA), antioxidant enzyme activities (CAT, SOD and GSPx) and T-AOC, were determined at an animal level. In serum, compared with the control group, AOP supplementation significantly increased the activities of SOD and GPx ($P < 0.05$). There was no significant difference between AOP and control group on the levels of T-AOC, CAT and MDA (Table 7).

The activities of antioxidant enzymes in liver and the corresponding gene expressions were shown in Table 7. Compare to

Table 8 Alpha diversity indexes of cecal bacteria in rats among different groups^a

Estimators	CON	AOP	<i>P</i> -value
Sobs	412.50 ± 25.27	426.17 ± 19.66	0.32
Shannon	3.44 ± 0.14 ^B	3.96 ± 0.29 ^A	0.002
Simpson	0.11 ± 0.02	0.08 ± 0.03	0.12
Ace	438.59 ± 27.79	455.93 ± 14.14	0.20
Chao	443.67 ± 30.07	459.02 ± 10.76	0.27
Coverage	0.99 ± 0.0001	0.99 ± 0.0002	0.86

^a Different letter within the same line denote significant differences between diets.

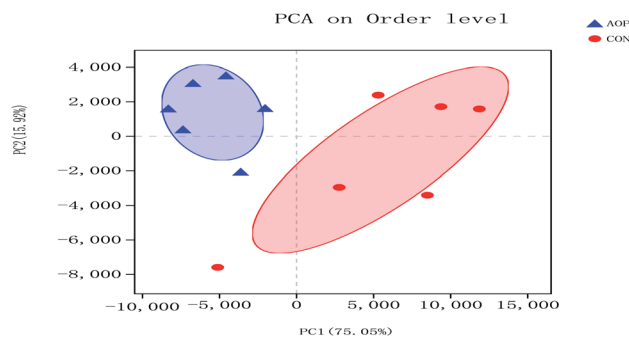


Fig. 7 Principal coordinate analysis (PCA) of caecum microbiome in rats in control group (CON) vs. polysaccharides group (AOP).

Wilcoxon rank-sum test bar plot on Phylum level

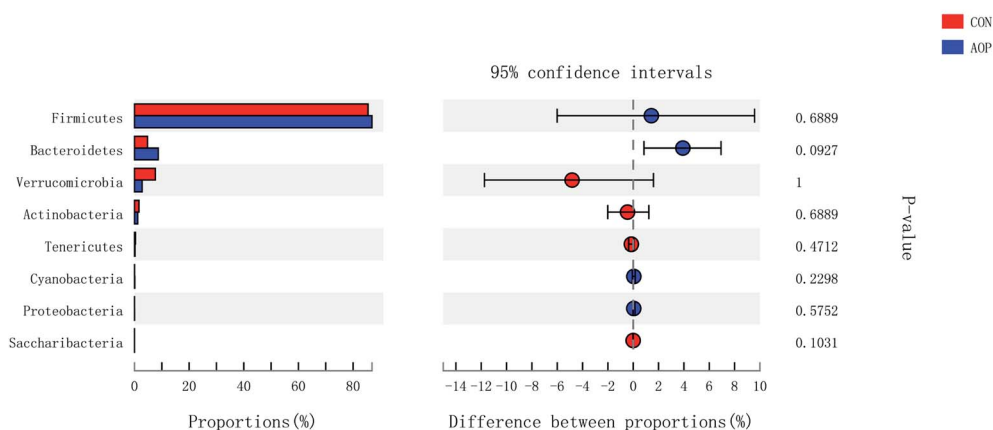


Fig. 8 Comparison of the bacteria (phylum level) present within the caecum of rats in CON and AOP groups.

those of control group, CAT and SOD activity of AOP group were increased, and the corresponding gene expressions (CAT, SOD1 and SOD2) were up-regulated with AOP addition as well ($P < 0.05$). In addition, AOP supplementation enhanced GPx activity ($P < 0.05$), however, the GPx gene expression didn't show significant difference between the two groups. The results indicated that AOP with remarkable antioxidant activity has important significance in natural medicine research and production.

3.8. Overall structural change of gut microbiota

3.8.1 Sequencing coverage and bacterial diversity. Twelve samples of caecum microbiome DNA ($n = 6$ for per group) were used to sequence the V3–V4 regions of the 16S rRNA gene by

Illumina Miseq sequencer after PCR and quality check with Agilent 2200 TapeStation and Qubit 2.0. Sequences shorter than 200 bp were removed, and 708 056 sequences were gained with an average length of 432 bp. A total of 555 OTUs were generated *via* clustering analysis for high-quality sequences at a 97% similarity cutoff. The rarefaction and Shannon index curves that were generated from the OTUs revealed that the data had covered most of the diversity and new phylotypes (Fig. 6), suggesting that high sampling coverage was captured with the sequencing depth, such that further increasing the sequencing depth was unlikely to achieve more gut microbiota diversity. Furthermore, the diets played a key role in shaping phylogenetic diversity based on the α -diversity. Thereinto, Shannon index

Wilcoxon rank-sum test bar plot on Genus level

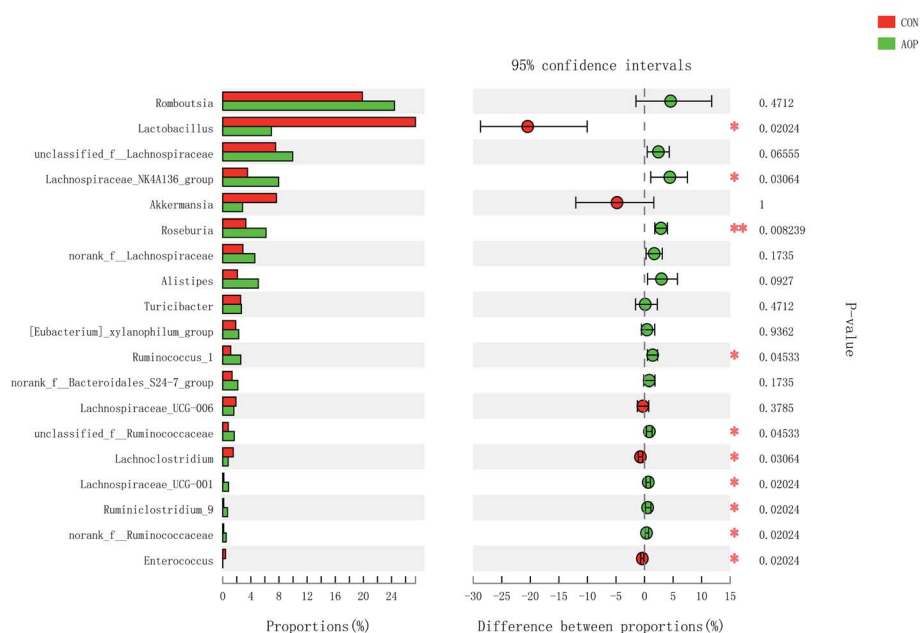


Fig. 9 Comparison of the bacteria (genus level) present within the caecum of rats in CON and AOP groups.

was significantly increased ($p < 0.05$) after AOP treatment (Table 8). The principal component analysis (PCA) was used to analyze the composition changes in the gut microbiota. The results revealed that AOP diet caused significant separation of fecal microbiota for CON and AOP diet groups (Fig. 7).

3.8.2 Changes in microbial composition after supplementation administration. Considerable studies showed that herbal medicine plants exerted beneficial ability against diseases by modulating gut microbiota.^{41,42} Hence, in order to investigate the structural response of gut microbiota to AOP feeding, the bacterial communities in rats were analyzed at the phylum and genus levels. At the phylum level, among the host microbiota, Firmicutes and Bacteroidetes were the predominant phyla in all treatment groups, followed by far less abundant Verrucomicrobia and Actinobacteria (Fig. 8). In general, gastrointestinal digestive enzymes can't digest polysaccharide. However, most of them can be fermented by gut microbiota. Short-chain fatty acids (SCFA) are main end products of the fermentation.^{43,44} High level of SCFA is unfavorable to several potentially

pathogenic bacteria,⁴⁵ but they can promote the proliferation of *Bacteroides*, *Ruminococcus*, *Lactobacillus*, *Prevotella*, and *Butyrivibrio*,^{46,47} thereby benefit the host. Unfortunately, short-chained fatty acids in hindgut were not detecting in this study. Based on previous study, polysaccharide can up-regulated short-chained fatty acids, stimulating the growth of beneficial microbes, such as Ruminococcaceae, *Bacteroidetes*, *Lactobacillus*⁴⁸ and *Prevotella*.⁴⁹ In the current study, AOP administration tended to increase the relative abundance of *Bacteroidetes* ($P = 0.09$). *Bacteroidetes* have been reported to be able to generate several SCFAs (e.g. acetic and propionic acid) by a range of glycoside hydrolases and carbohydrate metabolic pathways.⁵⁰ These results indicate that AOP presenting the growth of SCFA-producing bacteria in the gut, such as *Bacteroidetes*.

On genus level, the gut microbial community structure could be obviously changed by AOP feeding. In the present study, AOP increased the relative abundance of *unclassified_f_Lachnospiraceae* ($P = 0.06$), *Lachnospiraceae_NK4A136_group*

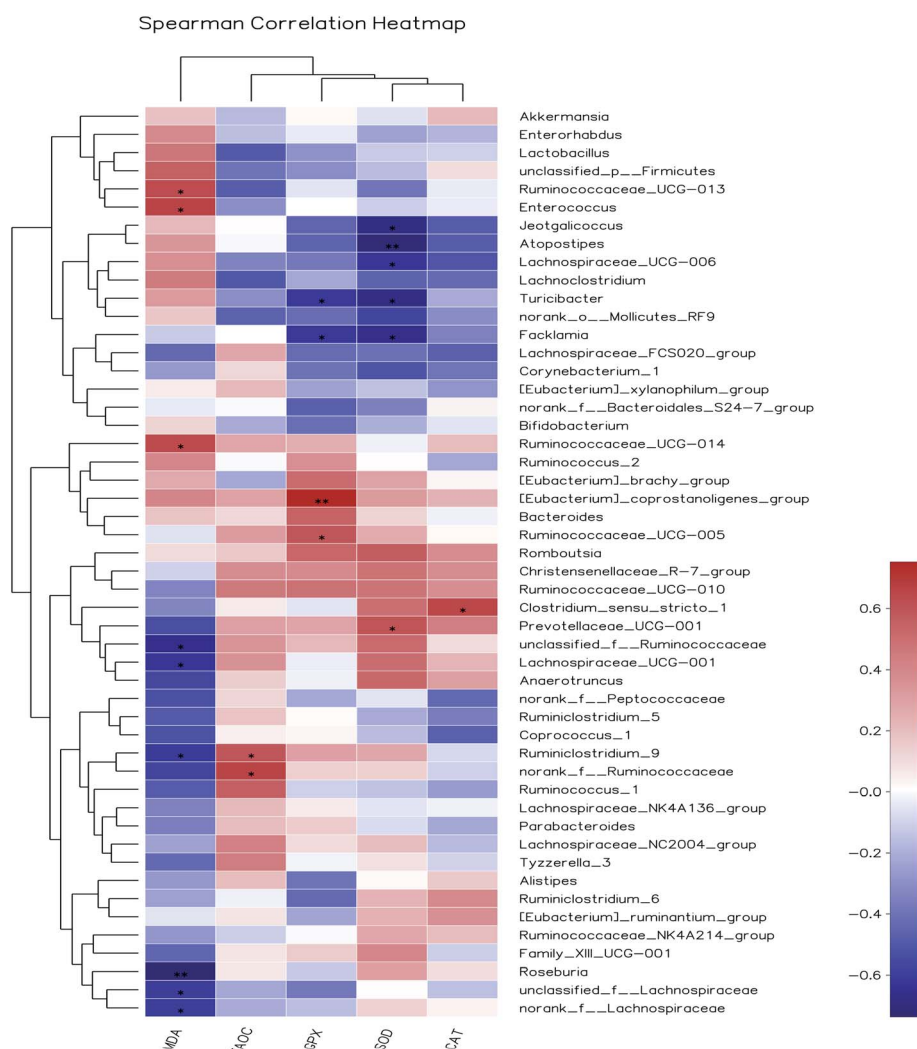


Fig. 10 Heat maps showing correlations between the relative abundance of sequences assigned to each bacterial genus and antioxidant indexes. Pearson's correlation coefficients (r) are given, with $r < 0$ indicating a negative correlation (blue), $r = 0$ indicating no correlation (white) and $r > 0$ indicating a positive correlation (red).

($P = 0.03$), *Roseburia* ($P = 0.008$), *Alistipes* ($P = 0.09$), *Ruminococcus_1* ($P = 0.04$), *unclassified_f_Ruminococcaceae* ($P = 0.04$), *Lachnospiraceae_UCG-001* ($P = 0.02$), *Ruminiclostridium_9* ($P = 0.02$) and *norank_f_Ruminococcaceae* ($P = 0.02$) and decreased the relative abundance of *Lactobacillus* ($P = 0.09$), *Lachnoclostridium* ($P = 0.09$) and *Enterococcus* ($P = 0.09$) (Fig. 9). The relative abundance of bacteria in the AOP group was significantly different, indicating that AOP fermentation played a significant impact on the microbial communities. This result is similar to the findings of Fu *et al.* (2018),²⁸ who reported that *Sargassum thunbergii* polysaccharide significantly increased the beneficial *Bifidobacterium*, *Roseburia*, *Parasutterella* and *Fusicatenibacter*. *Ruminococcus* and *Roseburia* have been well demonstrated to be the main butyric acid producers, responsible for degradation of polysaccharide and fibres.^{51,52} Therefore, AOP could potentially be a functional food modulating the composition and abundance of beneficial gut microbiota.

3.8.3 Correlation between gut bacteria and antioxidant indexes *in vivo*. Increasing evidences demonstrated that herbal medicines could modulate gut microbiota, thereby ameliorate inflammatory status and metabolic syndrome.⁵³ However, so far, limited studies have been done to illustrate the correlation between gut bacteria and antioxidant function. Pearson's correlation coefficient (r) was used to determine if any significant correlations could be observed between antioxidant indexes in serum of the rats fed the different diets and any of the most relatively abundant bacterial genera (Fig. 10). The MDA content was significantly and positively associated with the abundance of *Ruminococcaceae_UCG-013*, *Enterococcus* and *Ruminococcaceae_UCG-014*, while negatively correlated with *unclassified_f_Ruminococcaceae*, *Lachnospiraceae_UCG-001*, *Ruminiclostridium_9*, *Roseburia*, *unclassified_f_Lachnospiraceae* and *norank_f_Lachnospiraceae*. The T-AOC was positively correlated with members of the *Ruminiclostridium_9* and *norank_f_Ruminococcaceae*. The GPx activity was significantly and positively associated with the abundance of [*Eubacterium*]*_coprostanoligenes_group* and *Ruminococcaceae_UCG-005*, while negatively correlated with *Turicibacter* and *Facklamia*. SOD activity was positively associated with the abundance of *Prevotellaceae_UCG-001*, while negatively correlated with *Jeotgaliococcus*, *Atopostipes*, *Lachnospiraceae_UCG-006*, *Turicibacter* and *Facklamia*. CAT activity was positively associated with the abundance of *Clostridium_sensu_stricto_1*. Among them, the relative abundance of *unclassified_f_Ruminococcaceae* and *unclassified_f_Lachnospiraceae* were increased by AOP diets and negatively correlated with MDA content. Based on the present findings, we believed that the antioxidant effect of AOP was associated with the alteration of gut microbiota composition. Further in-depth research will be needed to understand the mechanism of cross-talk of gut microbiota and antioxidant function.

4. Conclusion

The optimum extraction conditions were as follows: a liquid–solid ratio of 15.4 : 1 mL g⁻¹, extraction time of 4.3 h, and extraction temperature of 60 °C. AOP, with a molecular weight of 2.1 kDa (62.6%) and 1.5 kDa (37.4%), has narrow polydispersity and rod conformations, and is composed of arabinose, galactose, glucose,

xylose, mannose, galacturonic acid and glucuronic acid monohydrate with molar ratio of 6.87 : 10.67 : 54.13 : 2.49 : 18.37 : 4.83 : 2.64 : 2.64. In addition, AOP could exert the ability to scavenge radicals *in vitro*. Furthermore, it was found that the AOP enhanced the activities of SOD, CAT, and GPx in the liver and serum of rats, and up-regulated the corresponding gene expressions. Moreover, AOP significantly modulated the composition of cecal bacterial populations. Therefore, AOP is expected to be a functional ingredient for health improvement through modulating the gut health.

Abbreviations

AOP	<i>Artemisia ordosica</i> polysaccharide
BBD	Box–Behnken design
RSM	Response surface methodology
GPC-	Gel permeation chromatography coupled to
MALLS-RI	multi-angle laser light scattering, a refractive index detection system
M_n	Number-average molecular weight
M_w	Weight-average molecular weight
TFA	Trifluoroacetic acid
DPPH	2,2-Diphenyl-1-picrylhydrazyl
ABTS	2,2'-Azinobis[3-ethylbenzothiazoline-6-sulfonic acid]-diammonium salt
RP	Reducing power
ADG	Average daily body weight gain
ADFI	Average daily feed intake
F/G	Ratio of feed to gain
ALT	Alanine aminotransferase
AST	Aspartate aminotransferase
ALP	Alkaline phosphatase
CAT	Catalase
SOD	Superoxide dismutase
GPx	Glutathione peroxidase,
T-AOC	Total antioxidant capacity
MDA	Malondialdehyde
RMS	Root mean square
PD	Polydispersity
PCA	Principal component analysis
SCFA	Short-chain fatty acids

Conflicts of interest

There are no conflicts to declare.

Acknowledgements

This work was supported by National Natural Science Foundation (Project No. 31960667).

References

- 1 C. W. Wright, *Artemisia*, New York, 1st edn, 2002.
- 2 K. Li, P. Zhang, B. Shi, J. Su, Y. Yue, M. Tong and S. Yan, Dietary *Artemisia ordosica* extract alleviating immune stress

- in broilers exposed to lipopolysaccharide, *Ital. J. Anim. Sci.*, 2017, **16**, 301–330.
- 3 Y. Xing, Y. Wu, C. Mao, D. Sun, S. Guo, Y. Xu, X. Jin, S. Yan and B. Shi, Water extract of *Artemisia ordosica* enhances antioxidant capability and immune response without affecting growth performance in weanling piglets, *J. Anim. Physiol. Anim. Nutr.*, 2019, **103**(6), 1848–1856.
- 4 X. Zhou, Y. Zhang, X. An, R. De Philippis, X. Ma, C. Ye and L. Chen, Identification of aqueous extracts from *Artemisia ordosica* and their allelopathic effects on desert soil algae, *Chemoecology*, 2019, **29**, 61–71.
- 5 C. W. Cho, C. J. Han, Y. K. Rhee, Y. C. Lee, K. S. Shin, J. S. Shin, K. T. Lee and H. D. Hong, Cheonggukjang polysaccharides enhance immune activities and prevent cyclophosphamide-induced immunosuppression, *Int. J. Biol. Macromol.*, 2015, **72**, 519–525.
- 6 N. Li, L. Li, J. C. Fang, J. H. Wong, T. B. Ng, Y. Jiang, C. R. Wang, N. Y. Zhang, T. Y. Wen and L. Y. Qu, Isolation and identification of a novel polysaccharide–peptide complex with antioxidant, antiproliferative and hypoglycaemic activities from the abalone mushroom, *Biosci. Rep.*, 2012, **32**, 221–228.
- 7 L. J. Li, M. Y. Li, Y. T. Li, J. J. Feng, F. Q. Hao and L. Zhang, Adjuvant activity of *Sargassum pallidum* polysaccharides against combined new castle disease, infectious bronchitis and avian influenza inactivated vaccines, *Mar. Drugs*, 2012, **10**, 2648–2660.
- 8 P. Zhang, B. Shi, T. Li, Y. Xu, X. Jin, X. Guo and S. Yan, Immunomodulatory effect of *Artemisia argyi* polysaccharide on peripheral blood leucocyte of broiler chickens, *J. Anim. Physiol. Anim. Nutr.*, 2018, (Suppl. 1), 1–8.
- 9 C. Ye and Y. Lai, Optimization of extraction process and antioxidant activity of polysaccharides from leaves of *Artemisia argyi* Levl. et vant, *J. Food Process. Preserv.*, 2015, **39**, 1309–1317.
- 10 H. J. Flint, E. A. Bayer, M. T. Rincon, R. Lamed and B. A. White, Polysaccharide utilization by gut bacteria potential for new insights from genomic analysis, *Nat. Rev. Microbiol.*, 2008, **6**, 121–131.
- 11 P. Louis, K. P. Scott, S. H. Duncan and H. J. Flint, Understanding the effects of diet on bacterial metabolism in the large intestine, *J. Appl. Microbiol.*, 2007, **102**, 1197–1208.
- 12 T. W. Hand, I. Vujkovic-Cvijin, V. K. Ridaura and Y. Belkaid, Linking the microbiota, chronic disease, and the immune system, *Trends Endocrinol. Metab.*, 2016, **27**(12), 831–843.
- 13 M. Dubois, K. A. Gilles and J. K. Hamilton, *Anal. Chem.*, 1956, **28**, 350–356.
- 14 M. M. Bradford, *Anal. Biochem.*, 1976, **72**, 248–254.
- 15 P. Siddhuraju and K. Becker, *J. Agric. Food Chem.*, 2003, **51**, 2144–2155.
- 16 T. Bitter and H. M. Muir, *Anal. Biochem.*, 1962, **4**, 330–334.
- 17 T. Di, G. Chen, Y. Sun, S. Ou, X. Zeng and H. Ye, Antioxidant and immune-stimulating activities in vitro of sulfated polysaccharides isolated from *Gracilaria rubra*, *J. Funct. Foods*, 2017, **28**, 64–75.
- 18 X. L. Wan, Y. Niu, X. C. Zheng, Q. Huang, W. P. Su, J. F. Zhang, L. L. Zhang and T. Wang, Antioxidant capacities of *Artemisia annua* L. leaves and enzymatically treated *Artemisia annua* L. in vitro and in broilers, *Anim. Feed Sci. Technol.*, 2016, **221**, 27–34.
- 19 Y. Wang, Z. Chen, J. Mao, M. Fan and X. Wu, Optimization of ultrasonic-assisted extraction process of *Poria cocos* polysaccharides by response surface methodology, *Carbohydr. Polym.*, 2009, **77**, 713–717.
- 20 C. Wang, L. Xu, L. Huang, X. R. Li, W. Han, D. Liu, X. Cui and Y. Yang, Optimization of maca polysaccharide extraction process and its chemo-protective effects on cyclophosphamide-induced mice, *J. Food Process Eng.*, 2018, **41**, e12856.
- 21 S. Tsubaki, K. Oono, M. Hiraoka, A. Onda and T. Mitani, Microwave-assisted hydrothermal extraction of sulfated polysaccharides from *Ulva* spp. and *Monostroma latissimum*, *Food Chem.*, 2016, **210**, 311–316.
- 22 C. Chen, L. You, A. M. Abbasi, X. Fu and R. H. Liu, Optimization for ultrasound extraction of polysaccharides from mulberry fruits with antioxidant and hyperglycemic activity in vitro, *Carbohydr. Polym.*, 2015, **130**, 122–132.
- 23 Y. L. Yan, C. H. Yu, J. Chen, X. X. Li, W. Wang and S. Q. Li, Ultrasonic-assisted extraction optimized by response surface methodology, chemical composition and antioxidant activity of polysaccharides from *Tremella mesenterica*, *Carbohydr. Polym.*, 2011, **83**, 217–224.
- 24 X. Guo, X. Zou and M. Sun, Optimization of extraction process by response surface methodology and preliminary characterization of polysaccharides from *Phellinus igniarius*, *Carbohydr. Polym.*, 2010, **80**, 344–349.
- 25 J. Liu, Y. Sun, L. Liu and C. Yu, The extraction process optimization and physicochemical properties of polysaccharides from the roots of *Euphorbia fischeriana*, *Int. J. Biol. Macromol.*, 2011, **49**, 0–421.
- 26 L. Wang, H. M. Liu and G. Y. Qin, Structure characterization and antioxidant activity of polysaccharides from Chinese quince seed meal, *Food Chem.*, 2017, **234**, 314–322.
- 27 X. Yu, C. Zhou, H. Yang, X. Huang, H. Ma, X. Qin and J. Hu, Effect of ultrasonic treatment on the degradation and inhibition cancer cell lines of polysaccharides from *Porphyrha yezoensis*, *Carbohydr. Polym.*, 2015, **117**, 650–656.
- 28 X. Fu, C. Cao, B. Ren, B. Zhang, Q. Huang and C. Li, Structural characterization and, in vitro, fermentation of a novel polysaccharide from, *Sargassum thunbergii*, and its impact on gut microbiota, *Carbohydr. Polym.*, 2018, **183**, 230–239.
- 29 W. Burchard, in *Branched Polymers II. Advances in Polymer Science*, ed. J. Roovers, Springer, Berlin, Heidelberg, 1999, vol. 143, pp. 113–194.
- 30 L. Yang and L. M. Zhang, Chemical structural and chain conformational characterization of some bioactive polysaccharides isolated from natural sources, *Carbohydr. Polym.*, 2009, **76**, 349–361.
- 31 V. Salvador, C. Cherbut, J. L. Barry, D. Bertrand, C. Bonnet and J. Delort-Laval, Sugar composition of dietary fibre and short-chain fatty acid production during in vitro

- fermentation by human bacteria, *Br. J. Nutr.*, 1993, **70**, 189–197.
- 32 H. B. Wang, S. J. Wu and D. Liu, Preparation of polysaccharides from cyanobacteria *Nostoc commune* and their antioxidant activities, *Carbohydr. Polym.*, 2014, **99**, 553–555.
- 33 S. Q. Li and N. P. Shah, Antioxidant and antibacterial activities of sulphated polysaccharides from *Pleurotus eryngii* and *Streptococcus thermophilus* ASCC 1275, *Food Chem.*, 2014, **165**, 262–270.
- 34 P. Shao, X. X. Chen and P. L. Sun, Chemical characterization, antioxidant and antitumor activity of sulfated polysaccharide from *Sargassum horneri*, *Carbohydr. Polym.*, 2014, **105**, 260–269.
- 35 P. F. Zhang, B. L. Shi, J. L. Su, Y. X. Yue, Z. X. Cao, W. B. Chu, K. Li and S. M. Yan, Relieving effect of *Artemisia argyi* aqueous extract on immune stress in broilers, *J. Anim. Physiol. Anim. Nutr.*, 2016, **101**, 251–258.
- 36 S. Guo, J. Ma, Y. Xing, Y. Xu, X. Jin, S. Yan and B. Shi, *Artemisia annua* L. aqueous extract as an alternative to antibiotics improving growth performance and antioxidant function in broilers, *Ital. J. Anim. Sci.*, 2020, **19**, 399–409.
- 37 L. P. James, P. R. Mayeux and J. A. Hinson, Acetaminophen-induced hepatotoxicity, *Drug Metab. Dispos.*, 2003, **31**, 1499–1506.
- 38 J. Zhang, X. Wang, V. Vikash, Q. Ye, D. Wu, Y. Liu and W. Dong, ROS and ROS-Mediated Cellular Signaling, *Oxid. Med. Cell. Longevity*, 2016, **2016**, 1–18.
- 39 Z. J. Wang, J. H. Xie, S. P. Nie and M. Y. Xie, Review on cell models to evaluate the potential antioxidant activity of polysaccharides, *Food Funct.*, 2017, **8**, 915–926.
- 40 Z. Wang, J. Xie, Y. Yang, F. Zhang, S. Wang, T. Wu, M. Shen and M. Xie, Sulfated *Cyclocarya paliurus* polysaccharides markedly attenuates inflammation and oxidative damage in lipopolysaccharide-treated macrophage cells and mice, *Sci. Rep.*, 2017, **7**, 40402–40412.
- 41 X. Tong, J. Xu, F. Lian, X. Yu, Y. Zhao, L. Xu, M. Zhang, X. Zhao, J. Shen, S. Wu, X. Pang, J. Tian, C. Zhang, Q. Zhou, L. Wang, B. Pang, F. Chen, Z. Peng, J. Wang, Z. Zhen, C. Fang, M. Li, L. Chen and L. Zhao, Structural Alteration of Gut Microbiota during the Amelioration of Human Type 2 Diabetes with Hyperlipidemia by Metformin and a Traditional Chinese Herbal Formula: A Multicenter, Randomized, Open Label Clinical Trial, *mBio*, 2018, **9**, e02392-17.
- 42 J. H. Wang, S. Bose, S. K. Lim, A. Ansari, Y. W. Chin, H. S. Choi and H. Kim, *Houttuynia cordata* Facilitates Metformin on Ameliorating Insulin Resistance Associated with Gut Microbiota Alteration in OLETF Rats, *Genes*, 2017, **8**, 239–258.
- 43 G. R. Gibson and R. Fuller, Aspects of in vitro and in vivo research approaches directed toward identifying probiotics and prebiotics for human use, *J. Nutr.*, 2000, **130**, 391S–395S.
- 44 L. Montagne, J. R. Pluske and D. J. Hampson, A review of interactions between dietary fibre and the intestinal mucosa, and their consequences on digestive health in young non-ruminant animals, *Anim. Feed Sci. Technol.*, 2003, **108**, 95–117.
- 45 A. Salonen and W. M. de Vos, Impact of diet on human intestinal microbiota and health, *Annu. Rev. Food Sci. Technol.*, 2014, **5**, 239–262.
- 46 H. Yang, Y. Xiao, G. Gui, J. Li, J. Wang and D. Li, Microbial community and short-chain fatty acid profile in gastrointestinal tract of goose, *Poult. Sci.*, 2018, **97**, 1420–1428.
- 47 H. Yang, Y. Xiao, J. Wang, Y. Xiang, Y. Gong, X. Wen and D. Li, Core gut microbiota in jinhua pigs and its correlation with strain, farm and weaning age, *J. Microbiol.*, 2018, **56**, 346–355.
- 48 X. Wang, X. Wang, H. Jiang, C. Cai, G. Li, J. Hao and G. Yu, Marine polysaccharides attenuate metabolic syndrome by fermentation products and altering gut microbiota: an overview, *Carbohydr. Polym.*, 2018, **195**, 601–612.
- 49 Y. Wang, Y. Fei, L. Liu, Y. Xiao, Y. Pang, J. Kang and Z. Wang, *Polygonatum odoratum* Polysaccharides Modulate Gut Microbiota and Mitigate Experimentally Induced Obesity in Rats, *Int. J. Mol. Sci.*, 2018, **19**, 3587.
- 50 M. A. Mahowald, F. E. Rey, H. Seedorf, P. J. Turnbaugh, R. S. Fulton, A. Wollam and J. I. Gordon, Characterizing a model human gut microbiota composed of members of its two dominant bacterial phyla, *Proc. Natl. Acad. Sci. U. S. A.*, 2009, **106**, 5859–5864.
- 51 S. Hooda, B. M. V. Boler, M. C. R. Serao, J. M. Brulec, M. A. Staeger, T. W. Boileau and K. S. Swanson, Pyrosequencing reveals a shift in fecal microbiota of healthy adult men consuming polydextrose or soluble corn fiber, *J. Nutr.*, 2012, **142**(7), 1259–1265.
- 52 K. P. Scott, J. C. Martin, S. H. Duncan and H. J. Flint, Prebiotic stimulation of human colonic butyrate-producing bacteria and bifidobacteria, in vitro, *FEMS Microbiol. Ecol.*, 2014, **87**(1), 30–40.
- 53 J. M. Leiro, R. Castro, J. A. Arranz and J. Lamas, Immunomodulating activities of acidic sulphated polysaccharides obtained from the seaweed *Ulva rigida* C. Agardh, *Int. Immunopharmacol.*, 2007, **7**, 879–888.